Optical and Electrochemical Characterisation of Carbon Anodes with Varying Porosity and Coke Quality

Gøril Jahrsengene[1,2], Mahyar Farmahini Farahani[2], Hogne Linga[3] and Ann-Mari Svensson[2]

[1]SINTEF Industry, Trondheim, Norway
[2]NTNU Norwegian University of Science and Technology, Trondheim, Norway
[3]Hydro Aluminium AS, Årdal, Norway

Abstract

The performance of carbon anodes in aluminium production will depend on both the coke quality (impurities, structure) and the physical properties of the anode (density, permeability, electric resistivity). Here, a set of industrial anodes of different porosity and permeability, and a set of pilot scale anodes of different calcined petrol cokes (CPC) were evaluated with respect to the anode potential, voltage oscillations, and double layer capacitance. Electrochemical characterisation of anodes with different permeability showed that the voltage oscillations due to CO_2 bubble formation on the horizontal anode surface was inversely correlated to the permeability, with the highest oscillations observed for dense anodes. Evaluating pilot scale anodes with different source CPC (1.4-5.5 wt% S), no significant differences were observed for the overpotential in the absence of bubbles. The anode made from isotropic coke showed a significantly higher double layer capacitance than the anisotropic anodes, indicating better wetting properties towards the electrolyte.

Keywords: Carbon anode, Anode permeability, Voltage oscillations, Double layer capacitance

1. Introduction

During aluminium production, alumina (Al_2O_3) dissolved in cryolite reacts electrochemically with carbon in the prebaked carbon anode, producing aluminium and CO_2 [1]. The cell voltage is about 4 V, significantly higher than the reversible potential of the reaction. A significant fraction of the irreversible voltage losses is associated with the anode. The main contributions include the anode overpotential, resistance increase because of produced gas bubbles, and resistance of the anode material itself [2]. Prebaked anodes consist of calcined petroleum coke (CPC), coal tar pitch binder and recycled anode butts, and both the quality of the coke and the anode properties are assumed to affect the irreversible losses at the anode. Understanding what influences the cell voltage is important when searching to improve the overall process and reducing the cost.

In addition to raw material properties, the physical anode properties, like density, permeability, electrical conductivity, and strength are important for the cell performance. Anode grade coke (often referred to as sponge coke) have traditionally been characterised by low sulfur and metal content, a mixed optical structure, and an open porosity permitting good pitch penetration. The availability of regular anode coke is not following the high demand from the aluminium industry, so higher sulfur cokes are increasingly used in anode production. This is usually accompanied by higher metal impurity levels in the cokes as well. In addition, to meet the high demand, fuel grade cokes (typically spherical, dense, and isotropic particles) have been introduced [3, 4].

Today, anodes are typically produced from blends of sponge cokes with relatively high variations in sulfur, while holding the anode sulfur level relatively constant. More sulfur in the anodes will increase the SO_2 emissions unless sufficient scrubbing is installed at the smelters. Sulfur seems to have the positive effect of reducing the reactivity of the carbon towards the produced CO_2 [5, 6] and is therefore beneficial at moderate levels in the anodes. However, the metal impurities catalyse the unwanted reactions between anode, air, and CO_2 [7, 8], and needs to be controlled or

minimised to reduce reactivity and contamination of the primary aluminium. Isotropic cokes, with its very different structure, have significantly higher thermal expansion than the regular anode cokes. To avoid cracking of the anode, the potential for blending isotropic and anisotropic coke is limited. The maximum value of isotropic coke is believed to be in the 20 - 30 % range [4, 9, 10].

The anode potential consists of several components, several of which are also dynamically influenced by bubble evolution on the surface (hyperpolarisation) [1, 11, 12]. In Equation 1, the reversible potential E^{rev} refers to the CO_2 formation reaction and may be assumed to be independent of material properties. The concentration overpotential, η_c, is considered negligible in saturated melts, as well as being very small in industrial cells [1]. The reaction overpotential is associated with the charge transfer reactions and consists of two contributions. The first is η_r', the reaction overpotential when the surface is free of bubbles, and the second part η_h, represents the increased overpotential due to locally higher current density from partial screening of the anode surface by bubbles. The $I(R_s' + \delta R_s)$ is the term related to the electrical resistance in the system with a current I flowing through the cell, where the R_s' part is the series resistance with no bubbles screening the surface and the δR_s part is the increase due to bubbles blocking the anode surface.

$$E_{\text{anode measured}} = E^{\text{rev}} + \eta_c + \eta_r{}' + \eta_h + I(R_s{}' + \delta R_s) \qquad (1)$$

In laboratory studies the different contributions to the cell potential can be investigated separately by suitably adapting the anode assembly. A horizontal anode assembly [12, 13] will maximise the bubble formation, and can be used to investigate the effect of hyperpolarisation. A vertical anode assembly [11, 14, 15] will minimise the bubble screening of the surface, and the reaction overpotential can be investigated without the effect of hyperpolarisation.

In this study, the horizontal anode assembly was used to investigate the voltage fluctuations caused by bubble formation on anodes with varying physical properties. For sufficiently small anodes used for laboratory scale experiments, the behaviour of the bubbles will result in a quasi-periodical dynamic pattern of voltage oscillations that can be evaluated [16]. In the second part, this study addresses the overpotential caused by material properties by looking at anodes with different types of CPC (1.4-5.5 wt% S) using a vertical anode assembly. The double layer capacitance, C_{dl}, is a measure of surface's ability to store electric charge by polarisation, and the area that is electroactive and wetted by the melt should be proportional to C_{dl}. This value was extracted using electrochemical impedance spectroscopy (EIS) [17].

2. Experimental

2.1 Materials and Anode Assembly

Anodes provided by Hydro Aluminium were used in this study. Cores were extracted from several anodes (A-E) and evaluated for further analysation based on the permeability (in-house Hydro method similar to ISO 15906:2007). Permeability, density (ISO 12985-1:2000) and specific electrical resistivity (ISO 11713:2000) are presented in Table 1, presenting some differences of properties within core from the same anode. Furthermore, anodes from a pilot study using smaller grains (<2 mm) and varying coke quality (sulfur in 1.4-5.5 wt% range, anisotropic and isotropic cokes) were also investigated as part of this study. These are referred to as anodes P1-P5 (these cokes have been thoroughly investigated in [18-20], in these papers referred to as cokes A-E). Anode P1 is presented in Table 1, while relevant sulfur and microstructural properties of the cokes are presented as part of the results (Table 3).

Table 1 – Permeability, density and specific electrical resistivity range of anodes used in the different parts for this study.

	Permeability (nPm)	Density (g/cm^3)	SER (μΩm)	Change in surface roughness	Horizontal assembly	Vertical assembly
A	1.17-1.57	1.584-1.600	51.7-56.4	X	X	
B	1.19-1.76	1.588-1.601	57.2-58.8	X	X	
C	0.77-1.29	1.595-1.609	52.5-56.1	X		
D	0.61-1.73	1.603-1.608	50.0-51.7	X		
E	0.45-0.54	1.618-1.623	55.0-60.5	X	X	
P1	3.53	1.557	61.3		X	X
P2	0.30	1.638	51.7			X
P3	0.57	1.627	51.1			X
P4	1.07	1.596	57.4			X
P5	2.79	1.588	48.7			X

10 mm core samples were drilled out from the larger cores extracted from the industrial anodes, and directly from the pilot anodes. Three different assemblies were used for the electrochemical measurements: unshielded anodes (electrochemical area 3.14 cm^2), horizontal assembly (1.10 cm^2) [12] and vertical assembly (1.57 cm^2) [11], where boron nitride was used as the shielding material.

2.2 Surface Characterisation

Surface topography was analysed using an Infinite Focus confocal microscope from Alicona. This method consists of scanning the area of interest by taking pictures over a certain height range, and then construct a 3D image of the surface. The vertical resolution was 100 nm. The surface roughness, including pits and other topography, was defined as the ratio between true and projected area (TA/PA).

The analysis was performed on several anodes as prepared before electrochemical testing to get an overview of the roughness and roughness variation between samples. The technique was also applied on a number of anodes after electrolysis, to investigate local consumption of the anode. The samples were ground to P#2000 using SiC paper before the electrochemical analysis, to facilitate identification of specific grains. After electrolysis the remaining electrolyte was removed by soaking in warm, saturated $AlCl_3$ solution before imaging

2.3 Electrochemical Measurements and Characterization

The electrochemical experiments were done in a closed furnace set-up similar to [11], using a Si_3N_4 shield in the bottom for the vertical anode assembly and no shield in the other experiments. The reference was made by placing 0.6 g Al in a BN container with a hole (to get contact with the melt) and a tungsten wire to achieve electrical contact. The carbon crucible acted as the counter electrode. The electrolyte was saturated with alumina, and a cryolite ratio of 2.3. Synthetic cryolite (≥ 97 %, Sigma Aldrich), an excess of 9.8 wt% AlF_3 (industrial grade, sublimed in-house), 9.4 wt% Al_2O_3 (99.4 %, Merck) and 4 wt% CaF_2 (≥ 97 %, Merck) was mixed. The experiments were performed in an argon atmosphere at 980 °C.

Two potentiostats were used for the electrochemical measurements. A Parstat 4000+ from Princeton Applied Research was used with a Bipolar Operational Power supply (amplifier) from Kepco for the horizontal and unshielded anode experiments. A Zahner IM6eX from Zahner-Elektrik (±2 A/4 V) was used for the vertical anode assembly.

Unshielded anodes were electrolysed at a constant current density of ~1 A/cm^2 for about 40 minutes, to investigate the wear (which was calculated to be approximately 0.5 mm) after electrolysis. For the horizontal anodes the electrochemical measurements consisted of two steps,

first electrolysis for 10 minutes at constant current density of 1 A/cm^2, following electrolysis at constant potential of 2.15 V for another 10 minutes (measurement frequency 100 Hz).

To evaluate the variations in voltage caused by bubbles, the voltage oscillations in the measured potential was extracted for five bubbles near the end of the 10 minutes. Faraday's law was used to calculate of the bubble volume, Equation 2, where I is the current, R is the gas constant, T is the temperature, n is number of electrons passed (4), and the pressure P is assumed to be 1 atm. A fast Fourier transform (FFT) was used on the last 2 minutes to extract the average each bubble used for growth and detachment, Δt, as this was more accurate than extracting the values from only five bubbles.

$$V_{\text{bubble}} = \frac{I \cdot \Delta t \cdot R \cdot T}{n \cdot F \cdot P} \qquad (2)$$

Similarly, the current oscillations using the constant voltage measurements can be used to calculate the bubble screening, Equation 3. Since the anode is small, the maximum current I_{max} is assuming the anode is completely free for bubbles [10, 13].

$$\text{Screening} = 1 - \frac{I_{min}}{I_{max}} \quad (3)$$

The anodes from the pilot scale study (P1-P5), were investigated with the vertical anode assembly. The samples were pre-conditioned for 6 minutes, cyclic voltammetry (CV) was done from OCP to 2.3 V before potentiostatic EIS spectra were recorded at OCP and in the 1.4-1.7 V region with AC amplitude of 50 mV.

All EIS data were fitted to equivalent electrical circuits using ZView 3.5f by Scribner Associates, Inc.. The series resistance R_s, *i.e.* the ohmic resistance resulting from resistivity of the electrolyte and resistance in the leads to the electrode, was extracted from the high frequency OCP spectra and used to correct the measured chronopotentiometry and CV data. A LR(Q(R(LR))) equivalent circuit [21], developed for the description of two-step electrochemical reactions with an adsorbed intermediate, was used to fit the impedance data. The equivalent circuit is provided in Fig. 1 (top), where L is the inductance in the external wires, R_s is the series resistance, Q is the constant phase element used to model a non-ideal double layer capacitance, $R_{ct,1}$ and $R_{ct,2}$ are the charge transfer resistances, and the L_{ads} is an inductance associated with the adsorbed intermediate species. The effective capacitance (C_{eff}), corresponding to the double layer capacitance, can be derived in accordance with Equation 4 [22]. The model in Fig. 1 includes two contributions from the constant phase element Q in Equation 4, where the α is the dimensionless constant of the Q (a value between 0 and 1 where 1 corresponds to an ideal capacitor).

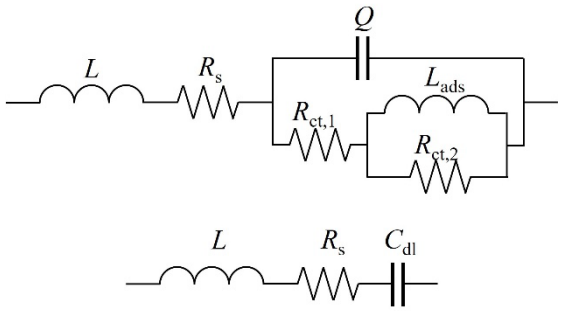

Fig 1 – The two equivalent circuits used to model the system and extract the capacitance, the LR(Q(R(LR))) and LRC circuits.

$$C_{\text{eff}} = Q^{1/\alpha}\left(\frac{R_s(R_{\text{ct},1}+R_{\text{ct},2})}{R_s+R_{\text{ct},1}+R_{\text{ct},2}}\right)^{(1-\alpha)/\alpha} \qquad (4)$$

The high frequency data was also used to extract the double layer capacitance, C_{dl}. At high frequencies no faradic reactions are assumed to occur and a simple LRC circuit can be used (bottom model in Fig. 1). The inductance L could be extracted from the imaginary impedance, Z_{Im}, at the highest frequency, f, (100000 Hz), as it may be assumed to be dominating at this frequency (Equation 5). The double layer capacitance C_{dl} can then be calculated (Equation 6). By definition, the double layer capacitance should be constant in this frequency region (100000-5000 Hz), but in practice the value is only constant for a limited frequency range, which varied between samples (method described in *e.g.* [23]). The capacitances, using both methods, were the reported in µF/cm^2.

$$L = L_{100000\text{Hz}} = \left(\frac{Z_{Im,\,100000\text{Hz}}}{2\pi f}\right) \qquad (5)$$

$$C_{\text{dl}} = \left(\frac{1}{2\pi f(2\pi f L - Z_{Im}}\right) \qquad (6)$$

3. Results and Discussion

3.1 Change of Surface Roughness during Electrolysis

Anodes A-E were investigated for this part of the study. Cores from four positions in each anode were investigated, with one unshielded anode fabricated from each core. After polishing the surface, the TA/PA did not vary significantly and was in the range 1.12-1.2 for all samples. No correlation was observed between these values and the anode properties. The small differences in the TA/PA are a result of the polishing, which have removed most of the features that could influence this value, and the physical properties was quite similar for all samples (0.5-1.8 nPm). Thus, all anodes had a relative similar surface before the electrochemical investigations.

The roughness after electrolysis increased with varying degree (5-35 % change in TA/PA), see Fig. 2. It is difficult to discern a correlation with the physical properties, but the change appears to be larger for the anode samples with the lowest permeability. The consistently high roughening of anode E (0.5 nPm) might indicate that part of the originally dense anode structure is being consumed quicker than the rest, most likely the binder phase.

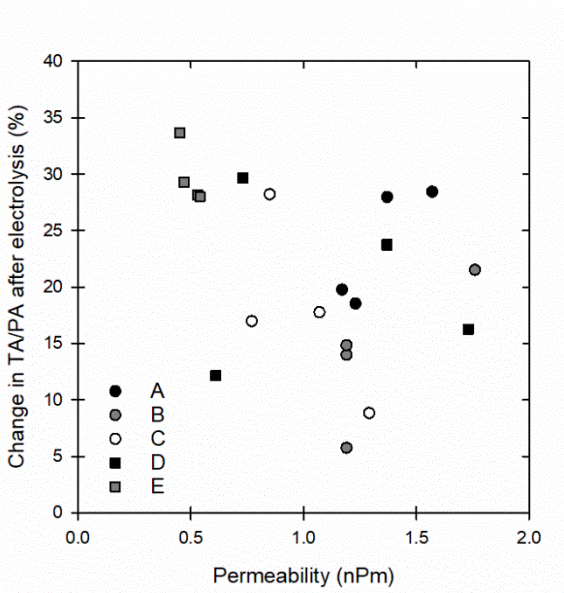

Fig. 2 – The wear during 40 minutes of electrolysis, presented as the increase in surface roughness (TA/PA) with respect to the permeability.

For some samples a bubble pattern was observed during the first part of the electrolysis. It appeared that the anodes with the lowest permeability had the largest variation in measured potential. More parallels with specific permeabilities and shielding of the vertical surface was needed to confirm these observations.

3.2 Electrochemical Analysis of Horizontal Surface – Bubble Behaviour

To avoid the bubbles forming at the vertical surface interfering with the measured voltage signals, the horizontal set-up was chosen for this analysis. A core from a singular position in the anodes A, B and E was chosen based the value for the permeability (0.5-1.7 nPm) and three parallels were investigated for each. Additionally, one of the pilot anodes having 3.5 nPm was part of the investigations (anode P1, coke with 1.4 wt% S). The anodes were polished and investigated for surface roughness before electrolysis, where a clear trend was observed in Fig. 3. The initial roughness is higher for the more permeable anodes, which also include one core from Anode C (not investigated further).

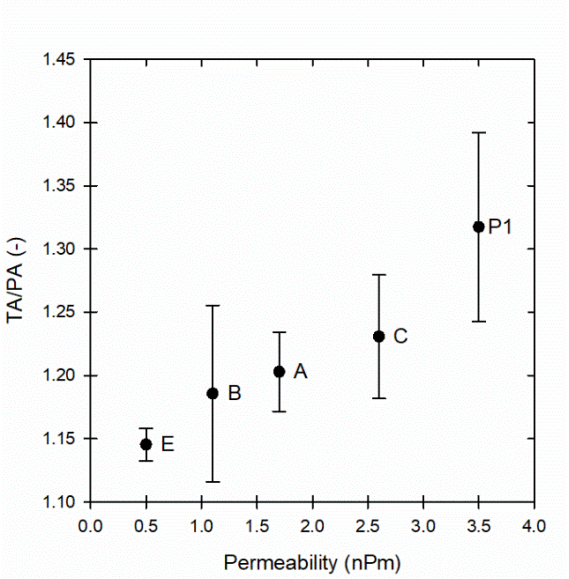

Fig. 3 – The roughness, expressed by TA/PA *vs* the anode permeability.

Examples of the voltage oscillations for graphite, Anode E (0.5 nPm) and Anode P1 (3.5 nPm) is presented in Figure 4, where the graphs have been shifted to an offset of 0 equal to when the anode has the lowest potential and is assumed to be without bubble coverage. The traditional saw-tooth pattern is observed for graphite, showing the largest bubble oscillations, and significantly larger than for the anode samples. This correlates well with previous investigations [10, 12]. For the anodes, the pattern shows bubbles varying in size, but the general saw-tooth pattern is observed also here. The less permeable Anode E had higher oscillations than Anode P1, with high permeability.

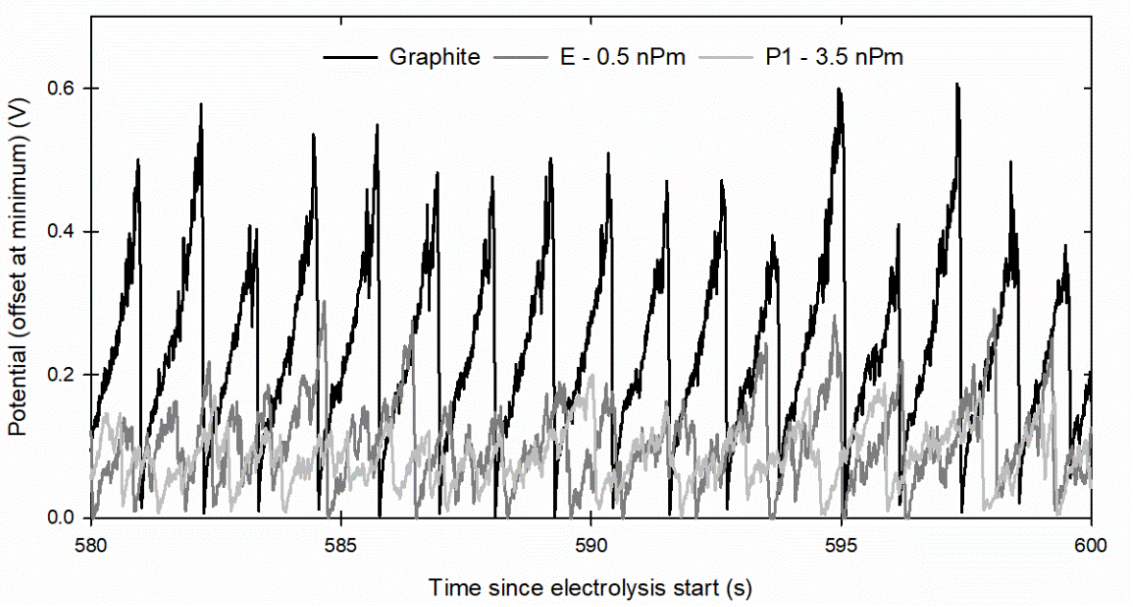

Fig. 4 – Examples of the measured potential vs time for graphite, the anode with lowest permeability and highest permeability. The graphs have been shifted to a similar offset (0).

Average values with its standard deviation (three parallels) of the voltage oscillation amplitude, bubble volumes (based on FFT analysis of the last two minutes of the constant current electrolysis data, extracting Δt for use in Faraday's law/Equation 2) and bubble screening of the surface (using the constant potential measurements and Equation 3) is presented in Table 2. The large standard deviation for some samples may be caused by inhomogeneity through the anode from which the sample originates, or simply because a small tilt in the set-up may facilitate faster bubble release.

Table 2 – Values for permeability, voltage amplitudes (extracted from measurements), CO_2 bubble volume (Faraday's law) and screening of the surface.

Material/Anode	Permeability (nPm)	Voltage amplitude (V)	Bubble volume (mL)	Screening of surface (%)
Graphite	-	0.51 ± 0.07	0.36 ± 0.02	60 ± 2
E	0.5	0.28 ± 0.10	0.37 ± 0.08	35 ± 4
B	1.1	0.22 ± 0.03	0.41 ± 0.05	39 ± 4
A	1.7	0.21 ± 0.05	0.44 ± 0.06	45 ± 3
P1	3.5	0.16 ± 0.02	0.70 ± 0.11	39 ± 5

The results show a clear correlation between the anode properties and the electrochemical behaviour when evaluating the CO_2 bubbles forming under the horizontal anode surface. The three industrial anode types have values quite close to each other, but the least permeable of these do have the highest oscillations. The pilot anode, with higher permeability than targeted for industrial anodes, exhibit the lowest oscillations due to bubbles. The bubble volumes are also very close for the three industrial anodes, with a significantly higher value for the highly permeable pilot anode. The values, 0.3-0.7 mL, are in a similar range as has been reported before using a similar set-up [12]. The bubble volumes appear to correlate with the voltage oscillation amplitudes, as increasing permeability correlates to lower amplitudes but larger volumes for each bubble. It does not appear to be a direct correlation with the screening calculated, as all values are in the 35-45 % range, similarly to what has been reported previously [10, 12]. The rough surface with several larger pores resulting from the more permeable anodes, appear to have a positive effect on how the gas bubbles are formed and released. Thorne *et al*. [12] evaluated if this was

because the gas could escape through the anode, but found, however, that this was unlikely. The effect is therefore more likely to be related to pores acting as nucleation sites, and that fact that the surface is rougher, while here, the screening is evaluated with respect to the geometric surface area. The bubbles formed on the highly permeable anodes needed longer before they detached resulting in a larger volume. Less permeable anodes have a smaller variation in voltage caused by blocking of anode surface than the more optimal, dense anodes. The graphite also behaves as expected based on previous literature [11], with high voltage amplitude, small bubble volume and large screening.

Considering the aluminium electrolysis process, for operational purposes, low amplitudes of the voltage oscillations are advantageous, however it appears that this might be at a cost of a less dense anode.

3.3 Electrochemical analysis of vertical surface – overpotential and capacitance

The vertical anodes made from cokes with different quality (P1-P5, relevant coke qualities are included Table 3) were investigated for overpotential and double layer capacitance. The resistance at OCP (R_{ct}) was used to *IR* correct the CV curves, resulting in graphs comparable to polarisation curves. Examples of graphite and three of the anodes are presented in Fig. 5. Graphite clearly have a higher overpotential at lower current densities than the anodes, in accordance with literature (see *e.g.* [11]). Anodes P1, P2 and P5 have marginally lower overpotential than anode P4 and P3. Three parallels of P1-P5 were investigated, showing an average potential about 0.06-0.08 V lower than for graphite. However, no significant differences in the overpotential for the anodes could be verified, as they were all within the standard deviations. Bubble oscillations on graphite is also visible in Fig. 5, indicating that minor bubble oscillations cannot be completely excluded on vertical electrode surfaces.

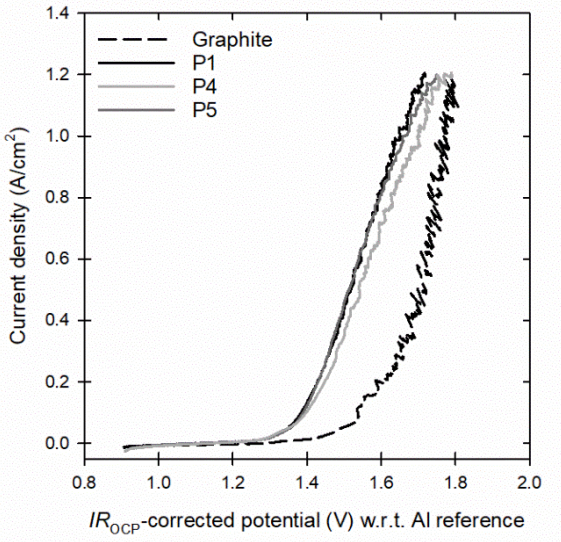

Fig. 5 – IR_{OCP} corrected CV curves of graphite, and anodes made of coke material P1 and P4 (anisotropic) and P5(E) (isotropic).

The Nyquist plots with the impedance raw data obtained at 1.5 V (not *IR*-corrected), and the modelled LR(Q(R(LR))) equivalent electrical circuit, is presented for anode P1 in Figure 6. The Nyquist plots appeared to be of the same quality for all the electrodes made from the pilot anodes, although the in-house electrode resulted in some differences between experiments done at different days. The LR(Q(R(LR))) model was used to estimate the effective capacitance, C_{eff}, from Q, in accordance with Equation. Due to the bubble noise, the graphite samples could not be fitted to the LR(Q(R(LR))) circuit. The simple LRC circuit was used to evaluate the high frequency data, assuming no Faradic reactions take place in this range, and the double layer capacitance, C_{dl}, was extracted. Both values are presented in Table 3 for the measurements at

1.5 V. C_{eff} is estimated lower than C_{dl}, but the trends are the same. The isotropic Anode P5 has a double layer capacitance, C_{dl}, significantly higher than the anisotropic anodes.

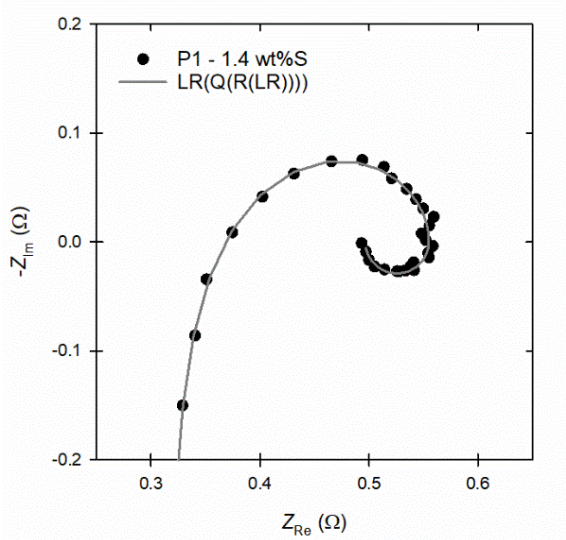

Fig. 6 – Example of the raw data from EIS at 1.5 V at anode P1, with the modelled equivalent circuit LR(Q(R(LR))).

Table 3 – The calculated effective capacitance C_{eff} using the LR(Q(R(LR))) circuit, and the double layer capacitance C_{dl} using the LRC circuit (1.5 V).

Material	Sulfur in coke (wt%)	Structure	C_{eff} (µF/cm^2)	C_{dl} (µF/cm^2)
Graphite	-	-	-	22 ± 7
P1	1.42	Anisotropic	64 ± 6	72 ± 6
P2	3.56	Anisotropic	70 ± 6	80 ± 4
P3	5.54	Anisotropic	52 ± 2	71 ± 3
P4	3.82	Anisotropic	60 ± 7	72 ± 7
P5	4.42	Isotropic	82 ± 5	95 ± 5

The simple LRC model do not rely on data in the low frequency region and was used on a larger collection of EIS spectra obtained at different voltages (1.4 V to 1.7 V). To better compare the results from different days (variations in reference electrode), C_{dl} is plotted against current density rather than potential. The result can be observed in Fig. 7, where the capacitance is relatively unchanged at lower current densities for all anodes. This is similar to the observations of Gebarowski *et al.* [14], where the capacitance stabilised at a voltage around 1.3 V, when current has reached a certain level. Fig. 7 also shows an increase in capacitance for several of the anodes at higher current densities; especially the isotropic Anode P5, which already have a significantly larger capacitance than the other anodes. The larger capacitance of the isotropic anode is comparable to what Sommerseth *et al.* [24] found, and the increase of capacitance for isotropic materials was also observed by Gebarowski *et al.* [14]. The significantly lower capacitance of graphite with respect to baked anodes was expected based on previous experimental observations [17, 24].

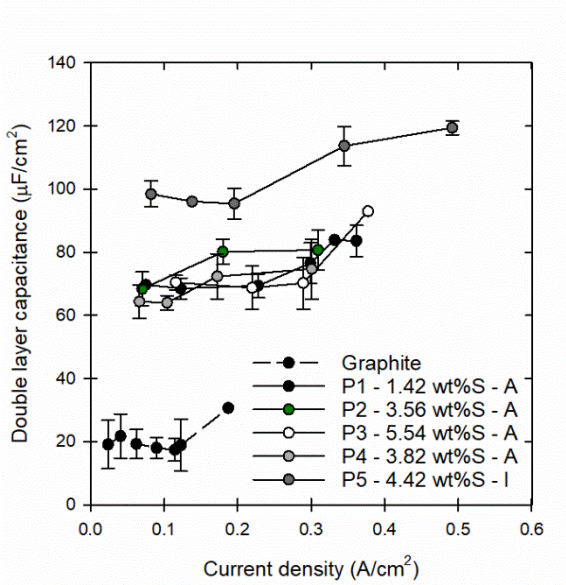

Fig 7 – The double layer capacitance estimated with the LRC circuit, *vs* the current density.

The results indicate that with respect to the electrochemical performance, no significant changes were observed between anisotropic anodes with varying sulfur levels, however, a positive effect on the capacitance was observed for the isotropic anode. Anode P1 had higher permeability than the other anisotropic anodes, but the higher roughness was not reflected in the double layer capacitance and electroactive area. This is probably a consequence of the fact that during the experiment, the pores are filled with gas, and not available for the electrochemical reaction. This was also the conclusion by Sommerseth *et al.* [25], who observed that electrolyte generally does not penetrate the pores on the surface.

4. Conclusions

Electrochemical characterisation of anodes with different permeability showed that the voltage oscillations due to CO_2 bubble formation on the horizontal anode surface appear to depend on the physical properties of the anode. Anodes with permeability of 0.5 nPm had significantly higher voltage oscillations than anodes in the 1.1-1.7 nPm range, which again was higher than the anode permeability of 3.5 nPm. The average voltage oscillations decreased from 0.28 V to 0.16 V from the lowest to highest permeability. Evaluating pilot scale anodes with different source CPC (1.4-5.5 wt% S), no significant differences were observed considering the reaction overpotential of all anodes. The anode made from isotropic coke showed a significantly higher double layer capacitance than the anisotropic anodes, indicating that addition of this coke type may be beneficial to the anode performance.

References

[1] Thonstad J *et al.* (2001), Aluminium Electrolysis: Fundamentals of the Hall-Héroult Process. Aluminium-Verlag, Düsseldorf

[2] Kvande H, Haupin W (2000) Cell Voltage in Aluminum Electrolysis: A Practical Approach. JOM 52(2):31-37

[3] Edwards L (2015) The History and Future Challenges of Calcined Petroleum Coke Production and Use in Aluminum Smelting. JOM 67(2):308-321

[4] Edwards L *et al.* (2012) Evolution of Anode Grade Coke Quality. Light Metals 2012, p 1204-1212

[5] Jones SS, Hildebrandt RD (1979) Influence of High-Sulfur Cokes on Anode Performance. Light Metals 1979, p 553-574

[6] Tran KN *et al.* (2009) Influence of Sulfur and Metal Microconstituents on the Reactivity of Carbon Anodes. Energy Fuels, 23(4):1909-1924
[7] Eidet T (1997) Reactions on Carbon Anodes in Aluminium Electrolysis. PhD Thesis, Norwegian University of Science and Technology
[8] Houston GJ, Øye HA (1985) Consumption of anode carbon during aluminium electrolysis. I-III. Aluminium 61:251-254, 346-349, 426,428
[9] Edwards L *et al.* (2009) Use of Shot Coke as an Anode Raw Material. Light Metals 2009, p 985-990
[10] Sommerseth C (2016) The Effect of Production Parameters on the Performance of Carbon Anodes for Aluminium Production. PhD Thesis, Norwegian University of Science and Technology
[11] Thorne RJ *et al.* (2015) Correlation between Coke Type, Microstructure and Anodic Reaction Overpotential in Aluminium Electrolysis. J. Electrochem. Soc. 162(12):E296-E307
[12] Thorne RJ *et al.* (2015) Bubble Evolution and Anode Surface Properties in Aluminium Electrolysis. J. Electrochem. Soc. 162(8):E104-E114
[13] Gebarowski W *et al.* (2017) Effect of Coke Properties on the Bubble Formation at the Anodes During Aluminium Electrolysis in Laboratory Scale. Light Metals 2017, p 1203-1211
[14] Gebarowski W *et al.* (2016) Interfacial Boundary between Carbon Anodes and Molten Salt Electrolyte. Light Metals 2016, p. 883-888
[15] Thorne RJ *et al.* (2014) Understanding Anode Overpotential. Light Metals 2014, p 1213-1217
[16] Kiss LI, Poncsák S (2002) Effect of the Bubble Growth Mechanism on the Spectrum of Voltage Fluctuations in the Reduction Cell. Light Metals 2002, p 217-223
[17] Kisza A, Thonstad J, Eidet T (1996) An Impedance Study of the Kinetics and Mechanism of the Anodic Reaction on Graphite Anodes in Saturated Cryolite-Alumina Melts. J. Electrochem. Soc. 143(6):1840-1847
[18] Jahrsengene G *et al.* (2019) Reactivity of Coke in Relation to Sulfur Level and Microstructure. Light Metals 2019, p 1247-1253
[19] Jahrsengene G *et al.* (2018) A XANES Study of Sulfur Speciation and Reactivity in Cokes for Anodes Used in Aluminum Production. Metall. Mater. Trans. B 49(3):1434-1443
[20] Jahrsengene G *et al.* (2019) An EXAFS and XANES Study of V, Ni, and Fe Speciation in Cokes for Anodes Used in Aluminum Production, Metall. Mater. Trans. B 50(6):2969-2981
[21] Harrington DA, Conway BE (1987) ac Impedance of Faradaic Reactions Involving Electrosorbed Intermediates—I. Kinetic theory. Electrochim. Acta 32(12):1703-1712
[22] Orazem M *et al.* (2013) Dielectric Properties of Materials Showing Constant-Phase-Element (CPE) Impedance Response. J. Electrochem. Soc. 160:C215-C225
[23] Jarek S, Thonstad J (1987) Double-layer capacitance and polarization potential of baked carbon anodes in cryolite-alumina melts. J. Appl. Electrochem. 17(6):1203-1212
[24] Sommerseth C *et al.* (2016) Electrochemical Reactivity and Wetting Properties of Anodes Made from Anisotropic and Isotropic Cokes, Light Metals 2016, p 865-870
[25] Sommerseth C *et al.* (2019) Electrochemical Behaviour of Carbon Anodes Produced with Different Mixing Temperatures and Baking Levels—A Laboratory Study. Light Metals 2019, p 1311-1318